Hauptseminar active matter
Microswimmers under confinement

Christoph Lohrmann

June 14, 2017

1 Introduction

When a boundary is nearby, the swimming trajectories of self-propelled active particles are greatly altered by the hydrodynamic interaction between the swimmer and the wall [1]. Boundary effects play a big role in many experiments, because in a microscope setup the microswimmers are confined between glass coverslips to get a high density of swimmers in the focal plane[2]. Additionally, artifical microswimmers are typically heavy and will sediment to the bottom surface of a containing vessel. In biology most microswimming takes place in confined geometries: Spermatozoa have to make their way through the confined reproductive tract and then stick to the ovum[3] and bacteria swim inside the host tissue. When it comes to the application of man-made active particles for drug delivery inside the body or as part of a lab-on-a-chip device, the main reason to use microswimmers instead of bigger ones is the small scale of the swimming environment.

It becomes clear that a theoretical understanding of the effects of boundaries on self-propelled microparticles is of great scientific interest.

2 Short review: Hydrodynamics

For the purpose of this review, the molecular level details of fluids can be neglected. The dynamics of a liquid is therefore described by a continuous flow field $\mathbf{u}(\mathbf{r}, t)$ governed by the Navier Stokes equation.

$$Re\left(\frac{\partial \mathbf{u}}{\partial t} + (\mathbf{u}\cdot\boldsymbol{\nabla})\mathbf{u}\right) = \boldsymbol{\nabla}\cdot\sigma + \mathbf{f}\ ,\ Re = \frac{u_0 L_0 \rho}{\eta} \tag{1}$$

The length and velocity scales that microswimmers operate on are very small; for example, an E. coli bacterium has a typical size of only about two micrometers and a maximum velocity of a few micrometers per second. In this regime, the Reynolds number that compares the influence of inertial and viscous forces on a flow field becomes very small, so the left terms of (1) can be

neglected and together with the assumption of an incompressible Newtonian fluid, one ends up with the Stokes equation

$$-\boldsymbol{\nabla} p + \eta \nabla^2 \mathbf{u} + \mathbf{f} = 0, \quad \boldsymbol{\nabla} \cdot \mathbf{u} = 0 \tag{2}$$

Eq. (2), in contrast to eq. (1), is linear in $\mathbf{u}$ so it can be solved using Green's functions. An arbitrary solution is a superposition of fundamental solutions which are called singularities or multipoles.

3 Pointlike description of microswimmers

The flow field a microswimmer induces in the surrounding fluid is generally very complex, however it can be decomposed into the fundamental solutions of the Stokes equation (2) that have a different decay with distance from the particle. When a swimmer first approaches a wall from the bulk liquid, the interaction is dominated by the most long ranged terms of the singularity expansion, the faster decaying ones can be neglected. In the far field, the flow field is approximated by a superposition of only a few terms of the singularity expansion. Including more terms increases the accuracy of the description, but many effects can be explained by considering only the first four:

$$\mathbf{u}(\mathbf{r}) = \alpha \mathbf{G_D}(\mathbf{r}; \mathbf{e}, \mathbf{e}) + \beta \mathbf{D}(\mathbf{r}; \mathbf{e}) + \gamma \mathbf{G_Q}(\mathbf{r}; \mathbf{e}, \mathbf{e}, \mathbf{e}) + \tau \mathbf{R_D}(\mathbf{r}; \mathbf{e}, \mathbf{e}) + \mathcal{O}\big(|\mathbf{r}|^{-4}\big) \tag{3}$$

$\alpha, \beta, \gamma, \tau$ are the expansion coefficients of each singularity and $\mathbf{e}$ is the orientation vector of the swimmer. The force dipole term $\mathbf{G_D}$ decays as $\sim 1/r^2$ and represents where the microswimmer generates its propulsive force: A swimmer as shown in fig 1 uses flagella behind the cell body to *push* itself through the surrounding fluid. This corresponds to $\alpha > 0$ in eq. (3). $\alpha < 0$ means the swimmer *pulls* itself. The other three terms decay as $\sim 1/r^3$. The source dipole term $\mathbf{D}$ represents the mass flow around the swimmer, the force quadrupole $\mathbf{G_Q}$ accounts for length asymmetries in the swimmer body and the rotlet dipole $\mathbf{R_D}$ describes the flow generated by microswimmers that use rotating flagella. There is no force or rotlet monopole because we assume that no external force and torque act on the particle and no source monopole because mass conservation prohibits the swimmer from constantly releasing fluid from its body.

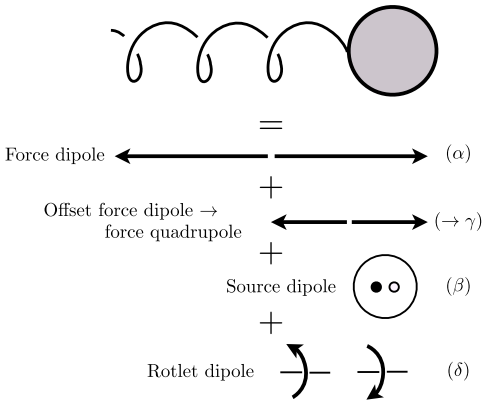

Figure 1: Example swimmer and the multipoles involved in the far field, from [4]

3.1 Hydrodynamic interaction with boundaries

Equation (3) describes the flow field generated by an active particle in free space. It is a solution of the Stokes equation (2) because it is a superposition of fundamental solutions and would be a valid description in an unbounded fluid. When, however, walls are present, additional boundary conditions have to be met. To compensate the flow of each singularity on a no-slip

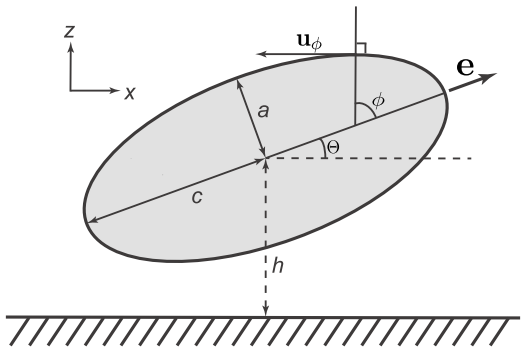

Figure 2: Variables used in this review, from [5]. h is the distance between the boundary and the center of the swimmer. Θ is the orientation angle, where $\Theta = 0$ means surface parallel swimming, $\Theta > 0$ an orientation pointed away from the wall and $\Theta < 0$ an orientation pointed towards the wall.

boundary, like in electrodynamics, mirror singularities (from now on denoted by a *) are placed at the image point $\mathbf{r_0^*} = \mathbf{r_0} - 2(\mathbf{r_0} \cdot \hat{\mathbf{n}})\hat{\mathbf{n}}$ outside the physical system. The mirror singularities affect not only the boundary but the whole system, especially the flow at the position of the microswimmer, which will consequently change its velocity $\mathbf{v}$ and orientation $\mathbf{e}$:

$$\mathbf{v}_{\text{tot}} = \mathbf{v} + \tilde{\mathbf{v}}, \quad \dot{\mathbf{e}} = \tilde{\boldsymbol{\Omega}} \times \mathbf{e} \tag{4}$$

The force and torque exerted on the swimmer can be computed from Faxén's laws. For spheroidal swimmers there is an exact analytical expression for Faxén's laws that results in the following additional translational velocity and rotational frequency of the swimmer:

$$\tilde{\mathbf{v}} = \mathbf{u}^*(\mathbf{r_0}) + \mathcal{O}\big(\nabla^2 \mathbf{u}^*|_{\mathbf{r_0}}\big) \tag{5}$$

$$\tilde{\boldsymbol{\Omega}} = \frac{1}{2}\boldsymbol{\nabla} \times \mathbf{u}^*(\mathbf{r_0}) + \Gamma \mathbf{e} \times (E^*(\mathbf{r_0})\mathbf{e}) + \mathcal{O}\big(\nabla^2(\boldsymbol{\nabla} \times \mathbf{u}^*)|_{\mathbf{r_0}}\big) \tag{6}$$

where

$$e = \frac{b}{a} \quad \text{ratio of half axes} \tag{7}$$

$$\Gamma = \frac{1 - e^2}{1 + e^2} \quad (= 0 \text{ for spheres}) \tag{8}$$

$$E^*_{ij} = \frac{1}{2}(\partial_i u^*_j + \partial_j u^*_i) \quad \text{strain rate tensor} \tag{9}$$

3.2 Decomposition of the boundary effects

Equations (5) and (6) are linear in $\mathbf{u}^*(\mathbf{x})$. Therefore the boundary effects of each term in the multipole expansion can therefore be evaluated separately and then added up in the end. The variables used throughout this review are shown in fig 2.

3.2.1 Force dipole

Evaluating (5) and (6) for the force dipole yields

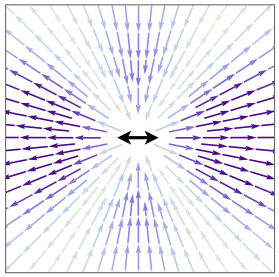

$$\tilde{v}_z = -\alpha \frac{3}{8h^2}(1 - 3\sin^2\Theta) \tag{10}$$

$$\dot{\Theta} = -\alpha \frac{3\sin(2\Theta)}{16h^3}\left(1 + \frac{\Gamma}{2}(1 + \sin^2\Theta)\right) \tag{11}$$

Figure 3: Force dipole flow field, from [4]

For a pusher ($\alpha > 0$) $\dot{\Theta}$ always has the opposite sign of Θ, so the torque acts to align the swimmer parallel to the wall. When it is swimming nearly parallel to the wall ($\sin\Theta < \frac{1}{\sqrt{3}}$), $\tilde{v}_z$ is negative, i.e. the swimmer is attracted to the wall.

A puller ($\alpha < 0$) will be aligned to be perpendicular to the wall, but in that case $\tilde{v}_z$ is also negative.

3.2.2 Source dipole

The wall-effects of the source dipole are

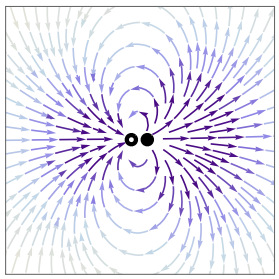

$$\tilde{v}_z = -\frac{\sin\Theta}{h^3} \tag{12}$$

$$\dot{\Theta} = \frac{3\cos\Theta}{8h^4}\left(1 + \frac{3\Gamma}{2}(1 + \sin^2\Theta)\right) \tag{13}$$

Figure 4: Source dipole flow field, from [4]

The swimmer is attracted to the wall if it is pointed away from it and repelled if it swims "nose down". $\dot{\Theta} > 0$ for all orientations means that the swimmer is always rotated away from the surface, even for $\Theta = 0$ where the force dipole causes no rotation.

3.2.3 Force quadrupole

The wall-effects of the force quadrupole are

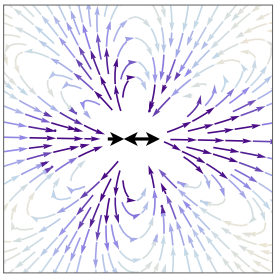

Figure 5: Force quadrupole flow field, from [4]

$$\tilde{v}_z = \frac{\sin\Theta}{4h^3}(7 - 9\sin^2\Theta) \tag{14}$$

$$\dot{\Theta} = -\frac{3\cos\Theta}{8h^4}\left(1 - 3\sin^2\Theta + \frac{\Gamma}{4}(11 - 3\sin^4\Theta)\right) \tag{15}$$

For small angles, the swimmer is attracted to the wall if it's pointed towards it and repelled if it swims "nose up". The sign of $\dot{\Theta}$ depends on the geometry of the swimmer represented by Γ, but for small angles $\dot{\Theta}$ is negative, so the swimming axis is rotated to point towards the wall. Both effects are the opposite of the source dipole contribution.

3.2.4 Rotlet dipole

The rotlet dipole term representing microswimmers propelled by rotating flagella doesn't have any effect on the wall attraction or rotation around axes parallel to the boundary

$$\tilde{u}_z = 0, \dot{\Theta} = 0. \tag{16}$$

Yet, it causes a different interesting effect:

$$\Omega_z = -\frac{3}{32h^4}\left(1 - 3\sin^2\Theta - \Gamma\cos^2\Theta(1 + 3\sin^2\Theta)\right) \tag{17}$$

The nonzero z-component of $\mathbf{\Omega}$ means that the swimmer is rotated around the z-axis resulting in a circular trajectory along the boundary.

3.2.5 Stochastic effects

The deterministic hydrodynamic effects described above compete with the random brownian motion caused by impacting molecules of the surrounding fluid. A timescale consideration helps to find the dominant effect [2]:

Hydrodynamic rotation The rotational frequency caused by the force dipole is

$$\Omega \sim \dot{\Theta} \sim \frac{\alpha}{h^3} \approx \frac{p}{\eta h^3} \tag{18}$$

where p is the physical dipole strength force times size of the particle. To move a particle with velocity U through a fluid with viscosity η, a force $f \approx \eta U L$ is needed, where L is the size of the particle. A swimmer located close to the wall ($h \approx L$) is consequently rotated on a timescale of

$$\tau_{\text{hyd}} \approx \Omega^{-1} \sim \frac{\eta L^3}{L \cdot \eta U L} = \frac{L}{U} \tag{19}$$

For the typical size and velocity of a microswimmer ($L = 10\,\mu\text{m},\ U = 20\,\mu\text{m}\,\text{s}^{-1}$) this results in the timescale for hydrodynamical rotation

$$\tau_{\text{hyd}} \approx 0.5\,\text{s}. \tag{20}$$

Diffusive rotation The timescale of the Brownian rotation can be obtained from the rotational diffusivity D_R:

$$\tau_{\text{diff}} \sim D_R^{-1} \sim \frac{\eta L^3}{k_B T} \approx 100\,\text{s} \gg \tau_{\text{hyd}} \tag{21}$$

The hydrodynamic dominates over the stochastic effect.

3.3 Full trajectories based on the pointlike description

In nature, trajectories can be observed [6] in which a bacterium gets hydrodynamically trapped by a wall, i.e. the particle approaches a surface and then continues on a trajectory along the boundary at a constant height above it. The goal of this section is to find a minimal description of a microswimmer using single multipoles to predict such a surface bound state.

3.3.1 Source dipole

For a swimmer described by only source dipole term, the dynamics is governed by the following two equations for the phasespace coordinates (h, Θ):

$$\dot{h} = \left(1 - \frac{\beta}{h^3}\right)\sin\Theta, \quad \dot{\Theta} = \frac{3\beta}{8h^4}\left(1 + \frac{3\Gamma}{2}\right)\cos\Theta \tag{22}$$

where the derivative of the height has one contribution from the free space swimming with unit velocity and an additional component from the force dipole - wall interaction. Integrating these coupled differential equations leads to the trajectories depicted in fig 6. We see that all trajectories are scattering trajectories no matter if the initial configuration is pointed away from the surface (square) or parallel (triangle) or pointed towards the surface (diamond).

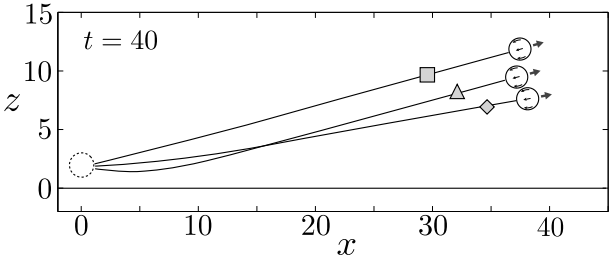

Figure 6: Trajectory of a force dipole with different initial conditions, from [4]

3.3.2 Force dipole

The dynamics of a force dipole follows this system of differential equations:

$$\dot{\Theta} = -\frac{3\alpha\sin(2\Theta)}{16h^3}\left(1 + \frac{\Gamma}{2}(1 + \sin^2\Theta)\right), \quad \dot{h} = \sin\Theta - \frac{3\alpha(1 - 3\sin^2\Theta)}{8h^2} \tag{23}$$

- $\alpha > 0$**: pusher** As discussed in section 3.2.1, the pusher is rotated parallel to the surface, so after some time $\Theta = 0$. The vertical velocity $\dot{h}(\Theta = 0) = -3\alpha/8h^2 < 0$, which means that the pusher impacts the wall. At this point, the description of a microswimmer only by a single multipole becomes invalid, because higher order singularities come into play and the geometry of the swimmer as well as possible electrostatic or chemical interaction between the surface of the boundary and the microswimmer become important.

- $\alpha < 0$**: puller** The puller gets rotated perpendicular to the wall, if the starting configuration was $\Theta_0 < 0$, after some time $\Theta = -\pi/2$. $\dot{h}(\Theta = -\pi/2) = -1 - 3|\alpha|/4h^2 < 0$ which also leads to an impacting trajectory

  If $\Theta_0 > 0$, after some time we have $\Theta = \pi/2$, $\dot{h}(\Theta = \pi/2) = 1 - \frac{3|\alpha|}{4h^2}$. For every α we can find a h so that $\dot{h} = 0$ which means that the swimmer hovers above the surface at a constant height. The problem is that this hovering state is unstable: If h is slightly bigger than its equilibrium value, $\dot{h} > 0$, so the swimmer won't be pulled back to the equilibrium position but will depart from the wall. If h is slightly smaller than the equilibrium value, the microswimmer will crash into the wall.

In all cases (source dipole, pusher, puller) the trajectories are scattering trajectories or trajectories that lead to wall impact. To find surface bound trajectories, one needs to look at the interplay between the different singularities, which becomes very tedious if done analytically, so for the next sections we leave the multipole approach and rely on numerical methods to model the swimmer and the flow fields in order to find trajectories.

4 Phasespace behaviour

An axisymmetric microswimmer that generates no rotational flow field can be described by only two variables: Its height h and Orientation Θ. Numerical simulations are used to find the flow field generated by the swimmer that fulfil all boundary conditions. From there we obtain the equation of motion and the trajectory in the phase space

$$\Rightarrow \begin{pmatrix} \dot{h} \\ \dot{\Theta} \end{pmatrix} = \mathbf{F}(h, \Theta), \quad \Rightarrow \begin{pmatrix} h(t) \\ \Theta(t) \end{pmatrix} \tag{24}$$

When looking for surface bound states there is special interest in stable fixed points (h^*, Θ^*) of that differential equation, because they correspond to "sliding" trajectories in physical space:

$$\mathbf{F}(h^*, \Theta^*) = \mathbf{0} \tag{25}$$

4.1 Squirmer model

The first model discussed here is that of a spheroidal squirmer. Microswimmers like Paramecium generate their propulsive flow by actuating thousands of small hairs (*cilia*) on their body surface. This mechanism can best be modelled by neglecting the single cilia and replacing their description by a constant slip velocity of the flow field on the swimmer surface. For the

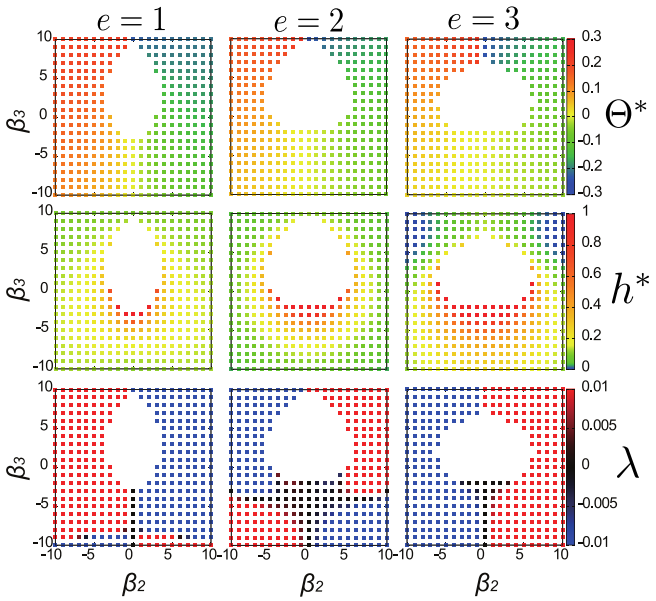

Figure 7: Fixed point values from [5]. e denotes the aspect ratio (ratio of the semi axes) of the spheroidal squirmer, β_2 and β_3 determine the strength of the V_2 and V_3 modes in the Legendre polynomial expansion of the slip velocity (negative β_2 corresponds to a *pusher*, positive to a *puller*, β_3 influences the higher order singularities in the far field). The first and second row depict the fixed point angle Θ^* and height h^*, respectively. The third row shows the stability of the fixed points (negative $\lambda \Leftrightarrow$ stable fixed point).

numerical approach[5], the tangent slip-velocity is expressed as a superposition of derivatives of the first three associated Legendre polynomials $V_n(x)$:

$$u_\phi(\phi) = \frac{3}{2}\left(V_1(\cos(\phi)) + \beta_2 V_2(\cos(\phi)) + \beta_3 V_3(\cos(\phi))\right) \tag{26}$$

where

$$V_n(x) = \frac{2\sqrt{1-x^2}}{n(n+1)}\frac{\mathrm{d}}{\mathrm{d}x}P_n(x), \quad P_n(x): \text{ Legendre polynomials} \tag{27}$$

For the definition of ϕ see fig 2. Comparing the far field effect of the slip-velocity (26) with the multipole ansatz (3) yields expressions for the multipole expansion parameters

$$\alpha = -\frac{3}{4}\beta_2 \quad \beta = \frac{1}{2} - \frac{1}{8}\beta_3 \quad \gamma = -\frac{5}{16}\beta_3 \tag{28}$$

Note that these equations are made dimensionless with V_1, R and η. The distinction between a pusher and a puller is encoded in β_2: $\beta_2 < 0 \Rightarrow \alpha > 0 \Rightarrow$ pusher, $\beta_2 < 0 \Rightarrow \alpha < 0 \Rightarrow$ puller.

4.1.1 Fixed points and limit cycles

The results depend strongly on the geometry of the swimmer as well as the modelled propulsive mechanism (pusher or puller) as shown in figure 7. For every aspect ratio e there is a region around $\beta_2 \approx 0$, $\beta_3 \approx 0$ where no fixed point can be found. An example of a swimmer characterized by these parameters is the spherical neutral squirmer. This type of swimmer can in good approximation be described solely by a source dipole, so the fact that there are no fixed points agrees with the results found in section 3.3.1. For the spherical squirmer ($e = 1$), where β_3 allows it, a puller ($\beta_2 < 0$) will swim stably along the wall with its nose pointed slightly downwards ($\Theta^* < 0$). For a more slender ellipsoidal shape only the pusher ($\beta_2 < 0$) has stable fixed points. In that case the fixed point angle is positive so the swimmer is pointed slightly away from the surface.

For the swimmers in the unstable region, the trajectories can be scattering trajectories with free space swimming for $t \to \infty$ as discussed in 3.3.

Another possibility in the unstable parameter region close to a stable fixed point is the occurrence of a limit cycle, where $(\dot{h}, \dot{\Theta})$ is never zero but the large time dynamics is not swimming in a straight line away from the wall but some stable periodic oscillation in $\phi(t)$ and $h(t)$ as illustrated in fig. 8.

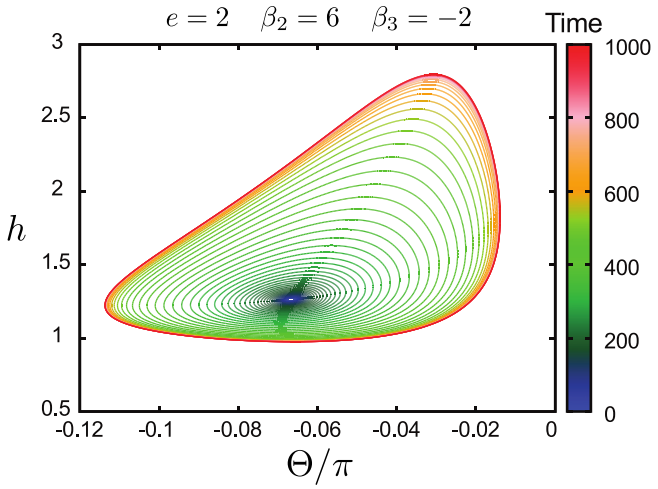

Figure 8: Limit cycle in a unstable parameter region, from [5]

Moving the parameters further into the unstable region increases the limit cycle until it intersects the wall, where the description becomes invalid.

4.2 Modelling via concentration gradient

A chemically active Janus particle induces a solute concentration gradient in the surrounding fluid by catalyzing a chemical reaction only on one side of its surface. This concentration gradient creates a flow that drives the swimmer forward. A description that assumes a constant slip velocity on the surface (as done in the squirmer) is not the most accurate. Instead the shape of the particle and the actual propulsion mechanism can be taken into account by numerically calculating the solute concentration around the swimmer due to a release of solute on the chemically active side. The results[7] match the outcomes of the previously discussed simulations:

A half covered Janus swimmer initially moving towards a wall will almost impact it, then be turned by hydrodynamic torques and eventually escape the surface independent of the initial conditions, just like the squirmer discussed in section 3.3. By altering the coverage, effectively the multipole expansion coefficients are changed and other states of motion can be achieved. Increasing the coverage enough qualitatively changes the phase space of the swimmer dynamics: A stable fixed point and a saddle point emerge. The stable fixed point corresponds to a sliding state, where the particle moves along the surface with a constant angle and height, like the pullers in 4.1.1. Increasing the coverage even further leads to a new "hovering" state: The swimmer points directly at the wall ($\Theta = -\pi/2$) and doesn't move along the surface, which is the same state as discussed in section 3.3.2, but in this case it is stable.

5 Summary

Walls influence the dynamics of microswimmers by the boundary conditions they impose on the flow field generated by the active particles. The change in the flow field due to the presence of a boundary is felt by the particle in the form of a force and a torque exerted on the swimmer by the flow field. The translational and rotational effects on the dynamics of a swimmer can be calculated from Faxén's laws.

An analytical far field description of a microswimmer using fundamental solutions of the Stokes equation can predict attraction to or repulsion from a boundary depending on the orientation of the swimmer. Trajectories of swimmers described by only a single fundamental solution always lead to scattering away from the surface or impacting it, where the far field description becomes invalid.

Using numerical methods to simulate microswimmers captures the interplay between all fundamental solutions as well as the geometry and propulsive machanism of the active particle, and makes reliable predictions even when the swimmer is very close to the wall.

Using the squirmer model (spheroidal swimmer described by a constant slip velocity on its surface) allows to find scattering and wall impacting trajectories as in the analytical approach but also reveals surface bound trajectories where the swimmer either slides along the boundary at constant height and orientation angle or oscillates within a finite distance from the wall.

Simulating a catalytically active Janus particle shows scattering and sliding trajectories as well as a new hovering state in which the swimmer doesn't move along the wall but stays in position pointed directly at the wall.

References

1. Lauga, E., DiLuzio, W. R., Whitesides, G. M. & Stone, H. A. Swimming in circles: motion of bacteria near solid boundaries. *Biophysical journal* **90,** 400–412 (2006).
2. Berke, A. P., Turner, L., Berg, H. C. & Lauga, E. Hydrodynamic attraction of swimming microorganisms by surfaces. *Physical Review Letters* **101,** 038102 (2008).
3. Cosson, J., Huitorel, P. & Gagnon, C. How spermatozoa come to be confined to surfaces. *Cell motility and the cytoskeleton* **54,** 56–63 (2003).
4. Spagnolie, S. E. & Lauga, E. Hydrodynamics of self-propulsion near a boundary: predictions and accuracy of far-field approximations. *Journal of Fluid Mechanics* **700,** 105–147 (2012).
5. Ishimoto, K. & Gaffney, E. A. Squirmer dynamics near a boundary. *Physical Review E* **88,** 062702 (2013).
6. Bianchi, S., Saglimbeni, F. & Di Leonardo, R. Holographic Imaging Reveals the Mechanism of Wall Entrapment in Swimming Bacteria. *Phys. Rev. X* **7,** 011010 (1 Jan. 2017).
7. Uspal, W., Popescu, M. N., Dietrich, S. & Tasinkevych, M. Self-propulsion of a catalytically active particle near a planar wall: from reflection to sliding and hovering. *Soft Matter* **11,** 434–438 (2015).